Extraction of Near-Field Fluorescence from Composite Signals to Provide High Resolution Images of Glial Cells

Robert T. Doyle,* Michael J. Szulzcewski,† and Philip G. Haydon*
*Carver Laboratory for Ultrahigh Resolution Biological Microscopy Department of Zoology and Genetics, Room 339 Science II, Iowa State University, Ames, Iowa 50011; and †Prairie Technologies, LLC, 3230 Deming Way, Middleton, Wisconsin 53562 USA

ABSTRACT The subdiffraction optical resolution that can be achieved using near-field optical microscopy has the potential to permit new approaches and insights into subcellular function and molecular dynamics. Despite the potential of this technology, it has been difficult to apply to cellular samples. One significant problem is that sample thickness causes the optical information to be comprised of a composite signal containing both near- and far-field fluorescence. To overcome this issue we have developed an approach in which a near-field optical fiber is translated toward the cell surface. The increase in fluorescence intensity during *z*-translation contains two components: a far-field fluorescence signal when the tip of the fiber is distant from the labeled cell, and combined near- and far-field fluorescence when the tip interacts with the cell surface. By fitting a regression curve to the far-field fluorescence intensity as the illumination aperture approaches the cell, it is possible to isolate near-field from far-field fluorescent signals. We demonstrate the ability to resolve actin filaments in chemically fixed, hydrated glial cells. A comparison of composite fluorescence signals with extracted near-field fluorescence demonstrates that this approach significantly increases the ability to detect subcellular structures at subdiffraction resolution.

INTRODUCTION

The principle of near-field microscopy was first described in 1928 by Synge, who suggested the possibility of extending the resolution of the light microscope by illuminating samples through a minute aperture that was significantly smaller than the wavelength of illuminating light (Synge, 1928). Ash and Nicholls (1972) put this method into practice using 3 cm radiation and a restricted aperture. Resolution equivalent to $\lambda/60$ was achieved. The use of a tapered optical fiber to provide restricted aperture illumination of samples has opened a new area of subdiffraction resolution imaging (Betzig and Chichester, 1992). Using optical fibers with apertures of the order of 50 nm, it has been demonstrated that single molecules could be interrogated to determine their physico-chemical properties (Sanchez et al., 1997; Xie and Dunn, 1994; Trautman et al., 1997; Betzig and Chichester, 1992, 1993). Despite the potential for high resolution imaging that near-field scanning optical microscopy (NSOM) provides, there have been few examples where this technique has been effectively utilized with biological specimens (Hwang et al., 1995, 1998; Subramaniam et al., 1998; Lewis et al.1999; Nagy et al.1999; Bui et al., 1999; Marchese-Ragona and Haydon, 1997; Valaskovic et al., 1997; Haydon et al., 1996; Moers et al., 1995; Hollars and Dunn, 1998; Sanchez et al., 1997). Although those that have been successful demonstrate that NSOM has the potential to revolutionize the biosciences (Hwang et al., 1995, 1998; Hollars and Dunn, 1998; Vickery and Dunn, 1999). The paucity of successful biological applications for NSOM probably arises because the original development of the technique was performed in the physical sciences, where the samples have very different characteristics from those in the life sciences.

Instead of being a planar sample on a coverslip, as is used in the physical sciences, cells have significant thickness, they must be imaged in solution, and, finally, they are highly compliant samples. Consequently, despite repeated attempts to image living or even chemically fixed and hydrated cells, little success has been achieved.

Because of the potential breakthroughs in understanding cell biology that might be achieved if we could image with 50 nm resolution, we have taken a different approach to performing NSOM. In this report we describe the development of a biological near-field microscope (BNFM), which achieves subdiffraction resolution on cells in solution.

MATERIALS AND METHODS

Cell culture

Enriched astrocyte cultures were produced from 1- to 3-day-old Sprague-Dawley rat cortices as previously described (Parpura et al., 1994). Briefly, cortices were dissected and the tissue was enzymatically (papain 20 IU/ml; Sigma, St. Louis, MO; 1 h at 37°C) and mechanically dissociated. The cells were plated into culture flasks and maintained at 37°C in humidified 5% CO_2/95% room air. After 7 to 13 days in vitro, the cells were shaken twice, first for 1.5 h and again after a change of media (cold) for 18 h on an orbital shaker at 260 rpm at 37°C. The enriched astrocytes were detached from the culture flask by incubation with trypsin (0.01%). The detached cells were diluted with modified minimal essential medium, collected by centrifugation (10 min at 750 rpm at room temperature), resuspended, and plated onto poly-L-lysine-coated 22 × 22 mm coverslips and maintained at 37°C in humidified 5% CO_2/95% room air.

Received for publication 28 August 2000 and in final form 13 February 2001.

Address reprint requests to P. G. Haydon, Carver Laboratory for Ultrahigh Resolution Biological Microscopy, Department of Zoology and Genetics, Room 339 Science II, Iowa State University, Ames, Iowa 50011. E-mail: pghaydon@iastate.edu.

0006-3495/01/05/2477/06 $2.00

Labeling of actin filaments

Cultured astrocytes were fixed with 4% formaldehyde in phosphate buffered saline (PBS) for 30 min at room temperature. The cells were then rinsed with PBS, permeabilized with 0.25% Triton X-100 PBS for 10 min, and blocked for 20 min with a PBS solution containing 5% bovine serum albumin (BSA), 5% normal goat serum, 0.25% Triton X-100, and 0.02% NaN_3. Actin filaments were labeled by either of two methods. Cells were exposed to Oregon green 488 phalloidin (Molecular Probes, Eugene, OR; 5U/ml in PBS with 0.5% BSA, 5% normal goat serum, 0.25% Triton X-100, and 0.02% NaN_3) for 20 min at room temperature. The staining solution was removed, the cells were rinsed three times with PBS, and they were ready for imaging. Alternatively, an anti-actin monoclonal antibody (Chemicon, Temecula, CA) was applied at a dilution of 1:100 in 0.5% BSA, 5% normal goat serum, 0.25% Triton X-100, and 0.02% NaN_3 overnight at 4°C. The cells were then rinsed three times (5 min) with 0.5% BSA, 5% normal goat serum, 0.25% Triton X-100, and 0.02% NaN_3 before application of a goat anti-mouse secondary antibody conjugated to Alexa Flour® 488 (Molecular Probes) for 1 hour at room temperature. The preparations were then rinsed with PBS before imaging.

Confocal microscopy was performed using a Prairie Technologies (Middleton, WI) confocal microscope. Post-image processing was performed using either Adobe Photoshop v4.0 or Metamorph software v4.1 (Universal Imaging Corp., Downingtown, PA)

Loading cells with calcein

To load cells with the indicator calcein, astrocytes were incubated for 5 min in saline solution containing 5 μg/ml of calcein AM (Molecular Probes). This indicator is insensitive to ion concentrations and is freely mobile in the cytosol.

Instrumentation

To perform our near-field studies, we developed an integrated near-field illumination positioning source with a confocal detection pathway (NeD_{NF}, Prairie Technologies) that is attached to a Nikon Diaphot 300 inverted microscope. Near-field optical fibers (50 nm reported aperture diameter, Topometrix, Santa Clara, CA or Nanonics, Jerusalem, Israel) were mounted on a triple axis motorized manipulator (25 mm movement in each axis) that also contained three axes of piezo-controlled movement (15 μm in each axis). Optical fibers were positioned above cells by visualizing the relative position of cells and the optical fiber with an ORCA digital camera (Hamamatsu, Japan) that was connected to one arm of our optical detection pathway. Using this system we were able to control the position of the near-field fiber with respect to the sample using calibrated software in which we could define the x and y image coordinates, and then command the motors to drive the optical fiber to the appropriate location. An aperture was then positioned at the secondary image plane, around the image of the tip of the near-field fiber. Positioning was performed by two motors that are calibrated such that aperture positioning is controlled from the camera image. After confirming the appropriate positioning of the aperture, a mirror was moved out of the optical pathway so that all photons were directed to a photomultiplier tube. The photomultiplier tube output was fed through a preamplifer to an integrator. To commence near-field studies we provided voltage ramps to the z piezo to extend the near-field fiber repeatedly toward the sample.

RESULTS

Previously, we demonstrated that the optical signal from a mobile fluorochrome within a cell can be used to monitor the relative positioning of a near-field optical fiber on a cell surface (Haydon et al., 1996). In our previous studies we performed measurements at single points of the cell. We have now extended this approach to permit linescan and imaging modalities. As an initial test of our system, we loaded astrocytes with the freely mobile dye, calcein, and asked whether we could reliably detect a fluorescence signal as the optical fiber was translated in the z axis toward the cell. Fig. 1 shows a wide-field image of cultured astrocytes loaded with calcein. We then switched to illumination through the near-field optical fiber and extended the fiber toward the cell. Fig. 1 *B* shows a typical fluorescence approach curve obtained during translation of the near-field fiber toward the cell. Note that this fluorescence signal is a composite signal of both far-field and near-field fluorescence. Initially the fluorescence signal is due to far-field illumination of the sample. However, as the fiber made contact with the cell surface, there was a nonlinear increase in fluorescence intensity due to local excitation of the sample by the evanescent wave at the tip of the near-field optical fiber.

Continued extension of the piezo caused no further increase in fluorescence, since the tip of the fiber is in contact with the cell surface. However, as reported previously (Haydon et al., 1996), when the piezo was extended for more than about 1 μm after contact, we observe an anomalous reduction in intensity during excessive translation of the fiber. The cause of this reduction in fluorescence intensity is not clear, but may result in part from a compression of the cell as well as from a disturbance of the evanescent wave at the tip of the optical fiber. For the purposes of this study, however, we have ignored this anomalous reduction in fluorescence, although we frequently extended the piezo to cause this reduction in intensity to serve as a reference point.

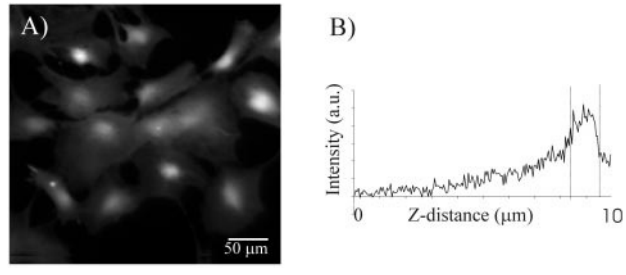

FIGURE 1 Translation of a near-field optical fiber to a calcein-loaded living glial cell demonstrates multiple fluorescent components. (*A*) A photomicrograph of a field of glial cells that are loaded with the indicator calcein. (*B*) Depiction of the relation between the fluorescent intensity of calcein and the z position of a near-field optical fiber that provides the excitation illumination. As the fiber approaches the cell from a distance, the intensity of fluorescence increases due to far-field illumination. However, as the tip of the optical fiber interacts locally with the cell surface, there is a nonlinear step in fluorescence intensity (*vertical dashed line*) due to local excitation of the fluorophore by the evanescent wave of the optical fiber. Continued translation of the fiber causes little change in intensity until an anomalous reduction in intensity as the cell is compressed.

For biological studies, where samples have significant thickness, composite far- and near-field fluorescence signals will be commonplace, and will hinder the potential resolution that can be achieved even with the smallest near-field aperture. To further test the utility of this approach, we turned to chemically fixed astrocytes in which the actin cytoskeletal network was labeled with Oregon green 488 phalloidin. In contrast to calcein-loaded cells, phalloidin-labeled actin filaments provide a non-uniform fluorescent sample (Fig. 2 *A*). *Z*-translation of a near-field optical probe to the surface of phalloidin-labeled astrocyte generates two types of fluorescence intensity curves. In the first, there is a relatively linear increase in fluorescence intensity as the tip approaches the cell surface (Fig. 2 *B*). In the second, there is this linear increase in far-field fluorescence until the fiber tip locally excites a phalloidin-labeled actin filament. Local excitation of the phalloidin-labeled actin filament by the evanescent wave causes a nonlinear increase in fluorescence intensity (Fig. 2 *C*). Since the increase in far-field fluorescence during *z*-translation of the optical fiber, is approximately linear, we reasoned that we could extract the far-field from the near-field fluorescence by using a linear regression curve. Consequently, for each *z*-translation we fit a linear regression curve to the data based on the slope calculated during the initial far-field fluorescence component. Fig. 2 *C* demonstrates that this approach does allow the selection of the nonlinear fluorescence component from the fluorescence curve that is acquired during translation of the optical fiber to the cell surface. Since this nonlinear component is not detected in unlabeled cells and is only obtained when the fiber approaches a labeled filament (as opposed to unlabeled regions of a cell), and since near-field fibers with a small aperture are required to detect this fluorescence, we suggest that it results from the local interaction of the evanescent component of the energy present at the tip of near-field optical fibers with the phalloidin-labeled actin filament.

To study further the utility of the extraction of near-field from far-field fluorescence data, we performed linescans on phalloidin-labeled astrocytes. Fig. 3 demonstrates the results of one such experiment. In this experiment, the *z* piezo

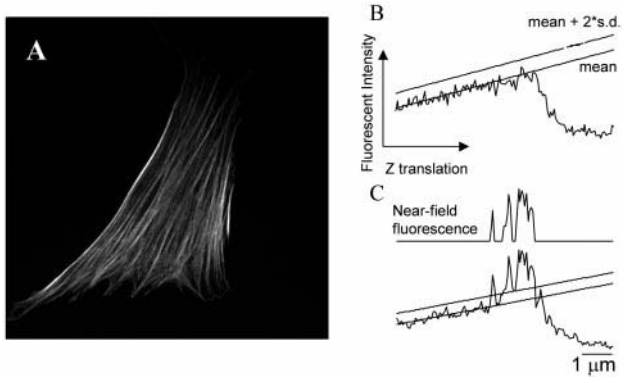

FIGURE 2 Oregon green 488 phalloidin-labeled actin filaments can be detected with near-field optical fibers. (*A*) A top view reconstructed confocal image of a glial cell that is labeled with Oregon green 488 phalloidin. (*B*) and (*C*) Relation between the fluorescent intensity of Oregon green 488 phalloidin and the *z* position of a near-field optical fiber. In (*B*) the fluorescence signal is shown when a near-field fiber approaches a region of an astrocyte that does not contain a labeled actin filament beneath the tip of the near-field optical fiber. Only a linear increase in fluorescence intensity due to far-field excitation is detected. By contrast (*C*), a step increase is fluorescence is detected when the evanescent wave of the near-field optical fiber illuminates a labeled actin filament. Superimposed on the data are two regressions corresponding to the linear regression of a baseline fit, as well as a linear regression that is offset by 2 standard deviations (SD) from the baseline. Note that as the tip interacts with the sample, the nonlinear increase in fluorescence exceeds these regressions. The upper trace represents the near-field fluorescence that was extracted from the composite signal (*lower trace*). Points that exceed the linear regression corresponding to the mean plus 2 SD for three consecutive points, were identified as due to evanescent excitation of the sample. Though one might normally use 3 SD as a criterion, we found that data which exceeded the mean plus 2 SD for three consecutive points was a more stringent way of isolating near-field data, because it prevented large transient spikes from being accepted as near-field data.

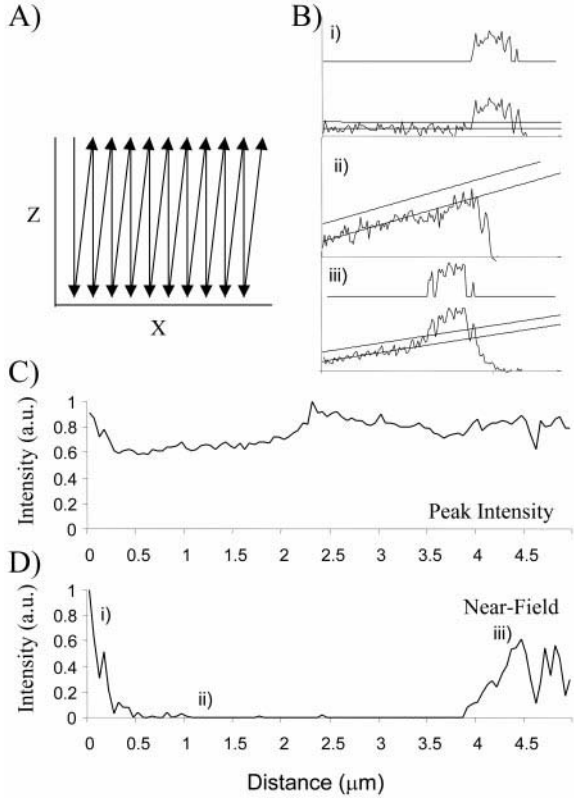

FIGURE 3 Linescan over bundles of actin filaments. (*A*) To perform a linescan over the surface of an Oregon green 488 phalloidin-labeled glial cell, the near-field fiber was translated in the *z* axis at each point along the line. (*B*) Three *z*-translation fluorescence curves are shown at three points along the line, labeled i, ii, and iii. (*C*) The peak fluorescence at each point is shown. (*D*) The intensity of the extracted near-field signal is shown. Note that the composite fluorescence signal in (*C*) shows little resolution of actin filaments, whereas after extraction of the near-field signal, distinct actin bundles can be resolved (*D*).

was translated toward the cell and the peak fluorescence intensity (composite near- and far-field fluorescence signal), as well as the extracted near-field fluorescence intensities, were determined. Then the *x* piezo was used to move the fiber to an adjacent region before a second *z*-translation was performed. By repeatedly performing *z*-translations of the optical fiber that were followed by moving an *x* increment (Fig. 3 *A*), we were able to generate intensities of fluorescence at each point on a linescan (Fig. 3 *B*). In the composite fluorescence signal (Fig. 3 *C*), little structural definition can be resolved due to the overwhelming contribution of far-field fluorescence to the composite signal. However, when the near-field fluorescence component is extracted (Fig. 3 *B*) during each *z*-translation and plotted on a normalized near-field linescan plot (Fig. 3 *D*), cross-sections of bundles of actin filament are now resolved. Using this method, it has been possible to resolve actin filaments with a resolution of about 50 nm (Fig. 4). Further validation of the utility of this approach is provided by a rare experiment in which the size of the aperture increased while performing a linescan. When the size of the aperture increased it was difficult to detect the nonlinear fluorescence component during *z*-translations of the optical fiber, and we were unable to detect structures with sub-diffraction resolution.

As a final test of this approach, we adopted an imaging mode in which each pixel in the *x* and *y* coordinates is generated by *z*-translations of the optical fiber. Fig. 5 shows an image of the peak fluorescence intensity (composite signal, Fig. 5 *A*) at each *x* and *y* pixel during a near-field imaging experiment and an image of the extracted near-field component of each pixel (Fig. 5 *B*). Clearly the use of a near-field extraction algorithm shows promise for permitting high resolution imaging of biological samples.

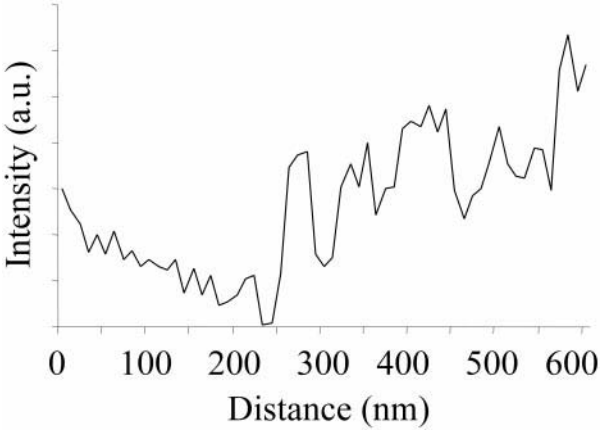

FIGURE 4 Linescan showing extracted near-field fluorescence intensity obtained from phalloidin-labeled astrocyte. A linescan was performed on a phalloidin-labeled astrocyte by performing sequential *z*-translations of the near-field optical fiber at 10 nm increments along the cell surface. Near-field fluorescence was extracted from total fluorescence using the linear regression method and is plotted at each *x* position. Intensities of fluorescence are shown on a linear scale with arbitrary units.

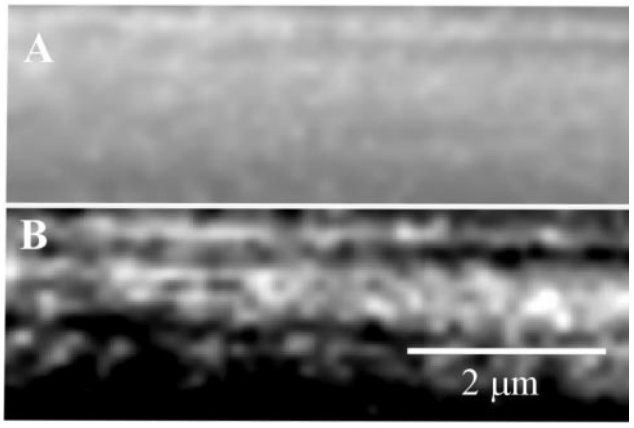

FIGURE 5 Composite fluorescence and near-field imaging of actin bundles. (*A* and *B*) 2 × 5 μm images that were generated over one actin bundle using a near-field optical fiber as the excitation source. (*A*) The peak intensity of fluorescence (composite of near and far-field fluorescence). (*B*) The extracted near-field fluorescence image. In these images, a 3 × 3 gaussian filter was used for display purposes.

DISCUSSION

In this study we have taken a novel approach to obtaining near-field optical data from cells. Instead of using shear-force feedback to maintain the near-field tip at a constant position with respect to the sample, we performed open loop experiments in which feedback per se is not employed. Rather, we use the fluorescent signal of the sample to provide the necessary information to obtain subdiffraction resolution structural data. Using both living and chemically fixed (hydrated) astrocytes, our studies show that the fluorescent signal generated by a near-field optical fiber is a composite of both far-field and near-field fluorescence. Although studies performed with single molecules or monolayers will not detect such a problem, this is a serious issue for biological imaging. Because cells have significant thickness, excitation energy that propagates to the far-field will illuminate distant fluorophore, causing a high background fluorescence signal upon which the near-field signal is superimposed. If this signal were constant, one could simply subtract a background level from a composite image to leave an uncontaminated near-field image. However, because this far-field component changes unpredictably across a cell, this approach is not feasible. Instead we demonstrate an alternative approach in which the relative contribution from far- and near-field fluorescence signals are identified at each pixel.

To identify the near-field component of a cellular fluorescence signal, we constructed approach curves in which the slope of the far-field fluorescence, during the *z*-translation of the near-field field optical fiber, is used to identify

the relative near- and far-field signals (Figs. 1–4). The validity of this method is demonstrated in several ways. We were unable to extract high-resolution near-field fluorescence when the aperture spontaneously enlarged during an experiment. When actin filaments were fluorescently labeled, *z*-translation of the optical fiber onto cells generated fluorescence curves consisting of either the far-field fluorescence (e.g., Fig. 2 *B*), or the composite near- and far-field fluorescence (e.g., Fig. 2 *C*). Finally, when calcein, a relatively homogeneously distributed fluorescent indicator, was loaded into astrocytes, we reliably detected both the near-field and far-field signals during each *z*-translation of the optical fiber, irrespective of its position over the cell.

One limitation of translating the near-field optical probe repetitively to the cell surface, in its current mode of operation, is that it is a relatively slow process that can take about 300 ms for each extension/retraction cycle. It should be possible, however, to increase the imaging speed by using higher vibration speeds and a lock-in approach in which the fluorescence intensity at two phases of the oscillation are taken as indications of the near-field and far-field fluorescence. With such an approach, we anticipate that it should be possible to generate 100 × 100 pixel images in about 10 s.

Much care and attention has been taken in developing high-speed, reliable feedback methods to control the positioning of near-field optical fibers over samples. Although these feedback methods are critical for studies in the physical sciences that employ hard samples, we now demonstrate that they are not necessary for studying living cells. One major difference between these two classes of study is the compliance of the sample under study. In the original studies in the physical sciences, contact between the tip and substrate instantly damages the aperture of the near-field optical fiber, immediately compromising optical resolution. However, since cells are soft, contact between the cell surface and the optical fiber rarely leads to aperture damage.

Our study of the use of near-field optical fibers to image living cells should now pave the way for a series of novel high-resolution investigations in cell and molecular biology. Since we can image at subdiffraction resolution, one can potentially investigate the distribution of membrane proteins and receptors, as well as other macromolecular entities. Perhaps even more exciting, however, is the opportunity to examine dynamic events in the cell cortex by illumination through the plasma membrane. This method will not, however, be able to probe at distances into the cell in a manner similar to confocal microscopy, since the nature of the evanescent wave restricts biological near-field microscopy to surface imaging. Nonetheless, for these surface measurements, near-field microscopy clearly surpasses confocal microscopy in *x*, *y*, and *z* resolution. We have now demonstrated that we can reliably position near-field optical fibers on living cells and, in parallel studies, have demonstrated that the fibers are non-invasive to the cells. Using the near-field extraction algorithm that has been developed in this study, it is anticipated that we will be able to record highly localized submembrane changes in ion concentration when using fluorescent ion indicators. Whereas evanescent wave or total internal reflection microscopy also reveals surface events such as vesicle dynamics (Zenisek et al., 2000), illumination through the near-field fiber provides increased *x, y* resolution, albeit at the expense of temporal resolution in imaging applications.

We thank Dr. M. McCloskey for comments on this manuscript.

This work was supported by funds from the National Institutes of Health to M.J.S. (MH57612) and P.G.H. (NS37585)

REFERENCES

Ash, E. A., and G. Nicholls. 1972. Super-resolution aperture scanning microscope. *Nature.* 237:510–512.

Betzig, E., and R. J. Chichester. 1992. Near-field optics: microscopy, spectroscopy, and surface modification beyond the diffraction limit. *Science.* 257:189–195.

Betzig, E., and R. J. Chichester. 1993. Single molecules observed by near-field scanning optical microscopy. *Science.* 262:1422–1425.

Bui, J. D., T. Zelles, H. J. Lou, V. L. Gallion, M. I. Phillips, and W. Tan. 1999. Probing intracellular dynamics in living cells with near-field optics. *J. Neurosci. Methods.* 89:9–15.

Haydon, P. G., S. Marchese Ragona, T. A. Basarsky, M. Szulczewski, and M. McCloskey. 1996. Near-field confocal optical spectroscopy (NCOS): subdiffraction optical resolution for biological systems. *J. Microsc.* 182:208–216.

Hollars, C. W., and R. C. Dunn. 1998. Submicron structure in L-alpha-dipalmitoylphosphatidylcholine monolayers and bilayers probed with confocal, atomic force, and near-field microscopy. *Biophys. J.* 75: 342–353.

Hwang, J., L. K. Tamm, Bohm, T. S. Ramalingam, E. Betzig, and M. Edidin. 1995. Nanoscale complexity of phospholipid monolayers investigated by near-field scanning optical microscopy. *Science.* 270: 610–614.

Hwang, J., L. A. Gheber, L. Margolis, and M. Edidin. 1998. Domains in cell plasma membranes investigated by near-field scanning optical microscopy. *Biophys. J.* 74:2184–2190.

Lewis, A., A. Radko, N. Ben Ami, D. Palanker, and K. Lieberman. 1999. Near-field scanning optical microscopy in cell biology. *Trends Cell Biol.* 9:70–73.

Marchese-Ragona, S. P., and P. G. Haydon. 1997. Near-field scanning optical microscopy and near-field confocal optical spectroscopy: emerging techniques in biology. *Ann. N. Y. Acad. Sci.* 820:196–206.

Moers, M. H. P., A. G. T. Ruiter, A. Jalocha, and N. F. Van Hulst. 1995. Detection of fluorescence in situ hybridization on human metaphase chromosomes by near-field scanning optical microscopy. *Ultramicroscopy.* 61:279–283.

Nagy, P., A. Jenei, A. K. Kirsch, J. Szollosi, S. Damjanovich, and T. M. Jovin. 1999. Activation-dependent clustering of the erbB2 receptor tyrosine kinase detected by scanning near-field optical microscopy. *J. Cell Sci.* 112:1733–1741.

Parpura, V., T. A. Basarsky, F. Liu, K. Jeftinija, S. Jeftinija, and P. G. Haydon. 1994. Glutamate-mediated astrocyte-neuron signalling. *Nature.* 369:744–747.

Sanchez, E. J., L. Novotny, G. R. Holtom, and X. S. Xie. 1997. Room-temperature fluorescence imaging and spectroscopy of single molecules by two-photon excitation. *J. Phys. Chem. A.* 101:7019–7023.

Subramaniam, V., A. K. Kirsch, and T. M. Jovin. 1998. Cell biological applications of scanning near-field optical microscopy (SNOM). *Cell Mol. Biol. (Noisy-le-grand).* 44:689–700.

Synge, E. H. 1928. A suggested method for extending microscopic resolution into the ultramicroscopic region. *Phil. Mag.* 6:356–362.

Trautman, J. K., J. J. Macklin, L. E. Brus, and E. Betzig. 1994. Near-field spectroscopy of single molecules at room temperature. *Nature.* 369:40–42.

Valaskovic, G. A., M. Holton, and G. H. Morrison. 1997. Biological near-field scanning optical microscopy: instrumentation and sample issues for shear-force feedback. *Ultramicroscopy.* 57:212–218.

Vickery, S. A., and R. C. Dunn. 1999. Scanning near-field fluorescence resonance energy transfer microscopy. *Biophys. J.* 76:1812–1818.

Xie, X. S., and R. C. Dunn. 1994. Probing single molecule dynamics. *Science.* 265:361–364.

Zenisek, D., J. A. Steyer, and W. Almers. 2000. Transport, capture and exocytosis of single synaptic vesicles at active zones. *Nature.* 406: 849–854.